Hydrothermal Microwave: A New Route to Obtain Photoluminescent Crystalline $BaTiO_3$ Nanoparticles

M. L. Moreira,[†] G. P. Mambrini,*[,†] D. P. Volanti,[⊥] E. R. Leite,[†] M. O. Orlandi,[‡] P. S. Pizani,[§] V. R. Mastelaro,[||] C. O. Paiva-Santos,[⊥] E. Longo,[⊥] and J. A. Varela[⊥]

LIEC, Departamento de Química, UFSCAR, Rod. Washington Luiz, km 235, P. O. Box 676, CEP 13565-905, São Carlos, SP, Brazil, Departamento de Física e Química, UNESP, P. O. Box 31, CEP 15385-000, Ilha Solteira, SP, Brazil, Departamento de Física, UFSCAR, P. O. Box 676, 13565-905, São Carlos, SP, Brazil, Instituto de Física, USP, P.O. Box 369, 13560-970, São Carlos, SP, Brazil, and LIEC, Instituto de Química, UNESP, R. Prof. Francisco Degni, s/n, P. O. Box 355, CEP 14801-907, Araraquara, SP, Brazil

Received February 19, 2008

Hydrothermal microwave method was used as a new route to synthesize pure $BaTiO_3$ (BT) nanoparticles at 140°C for 10 min under rapid reacting with stoichiometric Ba/Ti ratio. The crystalline products were characterized by X-ray powder diffraction (XRD) and the structure was refined by the Rietveld method from the tetragonal structure, which was supported by the Ti K-edge X-ray absorption near-edge structure (XANES). The pre-edge of Ti in the XANES spectra indicated that titanium ions are localized in a nonregular octahedron. Typical FT-Raman spectra for tetragonal $BaTiO_3$ nanoparticles presented well-defined peaks, indicating a substantial short-range order in the system. However, a scattering peak at 810 cm^{-1} was attributed to the presence of lattice OH^- groups, commonly found in materials obtained by hydrothermal process. Besides, the peak at 716 cm^{-1} can be related to eventual Ba^{2+} defects in the $BaTiO_3$ lattice. $BaTiO_3$ (BT) nanoparticles presented spherical morphology with a non-uniform distribution of particle sizes. An intense and broad photoluminescence band was observed around the green color emission at room temperature. By means of an excitation energy of 2.54 eV (488 nm), it was noted that the maximum profile emission (2.2 eV) is smaller than the forbidden band gap energy of $BaTiO_3$, indicating that certain localized levels within the band gap must exist.

Introduction

Barium titanate ($BaTiO_3$) is widely used for electronic devices in the technological ceramic industry because of its ferroelectric, thermoelectric, and piezoelectric properties when it assumes the tetragonal structure.[1] Its optical properties, particularly the luminescence of the nanostructured material, have attracted considerable attention.[2,3] Intense photoluminescence (PL) bands were reported for $BaTiO_3$ thin films[4] and powders synthesized by hydrothermal method, which was attributed to the recombination of self-trapped excitons in quasiamorphous materials.[4]

Direct generation of tetragonal $BaTiO_3$ (BT) nanoparticles by the hydrothermal process is of considerable interest due to its potential applications as a ferroelectric ceramic. However, the hydrothermal synthesis performed at temperatures below 240°C often yields cubic or pseudocubic barium titanate.[5] To convert the structure into tetragonal form, a new heat treatment at temperatures above 1000°C is required, which always leads to particle growth.[6] The tetragonal $BaTiO_3$ powders was directly prepared at temperatures between 450 and 600°C for several hours by a polymeric precursor type method.[6,7]

An alternative synthesis process, the hydrothermal microwave (HTMW) method, has recently been developed to prepare nanoparticles.[8–10] This is a genuine low temperature and high reacting rates method[11] due to direct interaction of radiation with mater. In the HTMW process, the introduction of electromagnetic microwave radiation offers significant advantages over the conventional process (CH). The fast reaction obtained in the microwave oven accelerates the crystallization process of the products by means of increasing the nucleation rate.[11,12] However, the barium titanate nano-

* Corresponding author. E-mail: mambrini@dq.ufscar.br.
[†] Departamento de Química, UFSCAR.
[‡] Departamento de Física e Química, UNESP.
[§] Departamento de Física, UFSCAR.
[||] Instituto de Física, USP.
[⊥] Instituto de Química, UNESP.

(1) Hennings, D.; Klee, M.; Waser, R. *Adv. Mater.* **1991**, *3*, 334.
(2) Zhang, W. F.; Yin, Z.; Zhang, M. S. *Appl. Phys. A* **2000**, *70*, 93.
(3) Takagahara, T.; Takeda, K. *Phys. Rev. B* **1992**, *46*, 15578.
(4) Pontes, F. M.; Pinheiro, C. D.; Longo, E.; Leite, E. R.; de Lazaro, S. R.; Magnami, R.; Pizani, P. S.; Boschi, T. M.; Lanciotti, F. *J. Luminesc.* **2003**, *104*, 175.
(5) Zhang, M. S.; Yin, Z.; Chen, Q.; Zhang, W.; Chen, W. *Solid State Commun.* **2001**, *119*, 659.
(6) Christensen, A. N. *Acta Chem. Scand.* **1970**, *24*, 2447.
(7) Kajiyoshi, K.; Ishizawa, N.; Yoshimura, M. *J. Am. Ceram. Soc.* **1991**, *74*, 369.
(8) Lu, S. W.; Lee, B. I.; Wang, Z. L.; Samuels, W. D. *J. Cryst. Growth* **2000**, *219*, 269.
(9) Chen, K. Y.; Chen, Y. W. *Powder Technol.* **2004**, *114*, 69.
(10) Keyson, D.; Volanti, D. P.; Cavalcante, L. S.; Simões, A. Z.; Sousa, I. A.; Vasconcelos, J. S.; Varela, J. A.; Longo, E. *J. Mater. Process. Technol.* **2007**, *189*, 316.
(11) Komarneni, S.; Roy, R.; Li, Q. H. *Mater. Res. Bull.* **1992**, *27*, 1393.
(12) Komarneni, S.; Rajha, R. K.; Katsuki, H. *Mater. Chem. Phys.* **1999**, *61*, 50.

10.1021/cm801638d CCC: $40.75
Published on Web 07/30/2008

particles prepared by this method (HTMW) at temperatures below 200°C, until now have presented only cubic structure.[13–16] Except in the method presented by Ma et al.[17] who prepared tetragonal $BaTiO_3$ in the presence of chloride ions in reaction time extending over several days, obtaining a *c*/*a* ratio equal to 1.008 in their products. However, the role of heating rates in the hydrothermal microwave method has not been well-discussed in the literature.

Photoluminescence is a powerful tool for investigating the energy levels, because this phenomena is related to the distribution of energy levels of materials.[18–22] Thus, it is one of the effective tools providing important information about materials physical properties at the molecular level, including shallow and deep defects and gap states.[23] Likewise, the photoluminescence behavior of crystalline $BaTiO_3$ synthesized by the hydrothermal microwave method has not yet been discussed in the literature; therefore, an approach regarding the structural order−disorder degree correlated to photoluminescence properties is befitting.

In this work, we have discussed favorable conditions to obtain intense and broad PL emission at room temperature for tetragonal $BaTiO_3$ nanoparticles synthesized by hydrothermal microwave method using low temperatures during short time and rapid reacting. The origin of the intense and broad PL band of $BaTiO_3$ samples were investigated in terms of electronic structure. Thus, characterization techniques were used as tools to investigate the order−disorder degree of $BaTiO_3$ samples.

Experimental Details

Synthesis. The $BaTiO_3$ (BT) nanoparticles were synthesized using $TiCl_4$ (99.95+ %, Aldrich), $BaCl_2\ 2H_2O$ (99%, Mallinckrodt) and KOH (p.a, Merck). Three solutions were prepared. In the first one, 0.05 mol of $TiCl_4$ was slowly added to 125 mL of deionized water at 0°C under stirring until it turned into a homogeneous solution. Similarly, 0.05 mol of $BaCl_2 \cdot 2H_2O$ was dissolved in 125 mL of deionized water. The two precursor solutions were mixed and separated into five portions, to which was added 50 mL of KOH solution (3 M) under constant stirring to act as a mineralizer, favoring the co-precipitation of the Ti and Ba hydroxides to form the reaction mixture as suggested by M. M. Kencka et al.[24]

The reaction mixture was placed in a 110 mL Teflon autoclave reaching 90% of its volume and providing maximum pressure efficiency,[25] which was sealed and placed in the HTMW system using 2.45 GHz microwave radiation with maximum power of 800 W.[26] The reaction mixture was heated to 140°C in less than 1 min (at 800W) and maintained at this temperature for 10 (BT10), 20 (BT20), 40 (BT40), 80 (BT80), and 160 (BT160) min under a constant pressure of 2.5 bar. After the reaction, the autoclave was naturally cooled to room temperature. Thus, the solid product was washed with deionized water several times and then dried overnight at 80°C.

Characterizations. The structural properties of the samples were characterized by X-ray diffraction (XRD) with a Rigaku DMax 2500 PC diffractometer, using Cu Kα radiation. Data were collected in step scanning mode, with 0.02° step size and 1 s/point, in a 2θ range from 10 to 120° with 0.5° divergence slit and 0.3 mm receiving slit. Crystal structures were identified and refined by the Rietveld method[27,28] using the TOPAS ACADEMIC v4.1 software.[29]

Raman spectroscopy was used to compare with XRD analyzes. Data were recorded on a Bruker RFS/100/S Fourier transform spectrometer (FT-Raman), with Nd:YAG laser excitation light at 1064 nm in a spectral resolution of 4 cm^{-1}. Inductively coupled plasma atomic emission spectrometer (ICP-AES) Varian VISTA MPX with radial configuration was used for chemical analyses. The generator frequency was 40 MHz, with RF power of 100 kW and plasma gas flow rate of 15 L min^{-1}. Emission bands at 455.4 and 366.1 nm were used to quantify barium and titanium content, respectively.

The titanium K-edge X-ray absorption spectra were collected at the LNLS (Laboratório Nacional de Luz Síncrotron) facility using the D04B-XAS1 beam line. The LNLS storage ring was operated at 1.36 GeV and 160 mA. XANES spectra of grounded samples were collected at the Ti K-edge (4966 eV) in transmission mode at room temperature using a Si(111) channel-cut monochromator. XANES (X-ray Absorption Near Edge Structure) spectra were recorded between 4910 and 5100 eV for Ti using energy steps of 0.5 eV. By comparison purposes among different samples, all spectra were background-removed and normalized using as unity the first EXAFS oscillation.[18]

Microstructural characterization was performed by field emission scanning electron microscopy (FE-SEM, Jeol JSM 6330F) and transmission electron microscopy (TEM, Jeol 3010 URP). Photoluminescence spectra were taken at room temperature with a U-1000 Jobin-Yvon double monochromator coupled to a cooled GaAs photomultiplier and a conventional photon counting system with 488.0 nm exciting and laser's maximum output power kept at 27 mW.

Results and Discussion

Figures 1 supports the nanometric nature (<100 nm) of barium titanate particles obtained by the hydrothermal microwave method under rapid heating (140°C/min), which present diameters between 25 and 80 nm. These values are inside of the range of distribution sizes corresponding to

(13) Newalkar, B. L.; Komarneni, S.; Katsuki, H. *Mater. Res. Bull.* **2001**, *36*, 2347.
(14) Liu, S. F.; Abothu, I. R.; Komarneni, S. *Mater. Lett.* **1999**, *38*, 344.
(15) G. J. Choi, G. J.; Kim, H. S.; Cho, Y. S. *Mater. Lett.* **1999**, *41*, 122.
(16) Sun, W.; Li, J.; Liu, W.; Li, C. *J. Am. Ceram. Soc.* **2006**, *89*, 118.
(17) Ma, Y.; Vileno, E.; Suib, S. L.; Dutta, P. K. *Chem. Mater.* **1997**, *9*, 3023.
(18) Lazaro, S.; de Milanez, J.; Figueiredo, A. T.; Longo, V. M.; Mastelaro, V. R.; Vicente, F. S.; de Hernandes, A. C.; Varela, J. A.; Longo, E. *Appl. Phys. Lett.* **2007**, *90*, 111904.
(19) Jan, J. C.; Kumar, K. P. K.; Chiou, J. W.; Tsai, H. M.; Shih, H. L.; Hsueh, H. C.; Ray, S. C.; Asokan, K.; Pong, W. F.; Tsai, M. H.; Kuo, S. Y.; Hsieh, W. F. *Appl. Phys. Lett.* **2003**, *83*, 3311.
(20) Pontes, F. M.; Longo, E.; Leite, E. R.; Lee, E. J. H.; Varela, J. A.; Pizani, P. S.; Campos, C. E. M.; Lanciotti, F.; Mastelaro, V.; Pinheiro, C. D. *Mater. Chem. and Phys.* **2003**, *77*, 598.
(21) Leite, E. R.; Paris, E. C.; Pontes, F. M.; Paskocimas, C. A.; Longo, E.; Pinheiro, C. D.; Varela, J. A.; Pizani, P. S.; Campos, C. E. M.; Lanciotti JR, F. *J. of Mater. Sci.* **2003**, *38*, 1175.
(22) Longo, V. M.; Cavalcante, L. S.; Figueiredo, A. T.; de Santos, L. P. S.; Longo, E.; Varela, J. A.; Sambrano, J. R.; Parkocimas, C. A.; Vicente, F. S.; de Hernades, A. C. *Appl. Phys. Lett.* **2007**, *90*, 091906.
(23) Schroder. D. K. *Semiconductor Material and Device Characteristics*; John-Wiley: New York, 1990.
(24) Lencka, M. M.; Riman, R. E. *Chem. Mater.* **1993**, *5*, 61.
(25) Walton, R. I. *Chem. Soc. Rev.* **2002**, *31*, 230.
(26) Volanti, D. P.; Cavalcante, L. S.; Keyson, D.; Lima, R. C.; Moura, A. P.; de Moreira, M. L.; Macario, L. R.; Godinho, M. *Met. Mater.* **2007**, *63*, 351.
(27) Rietveld, H. M. *Acta Crystallogr.* **1967**, *22*, 151.
(28) Rietveld, H. M. *J. Appl. Crystallogr.* **1969**, *2*, 65.
(29) Coelho, A. *Topas Academic*, 4.1 ed.; Coelho Software: Brisbane, Australia, 2007.

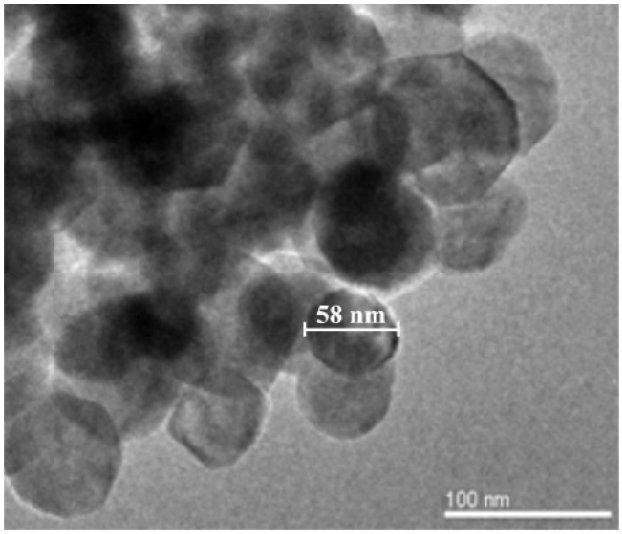

Figure 1. TEM image of spherical $BaTiO_3$ nanoparticles synthesized at 140°C for 10 min.

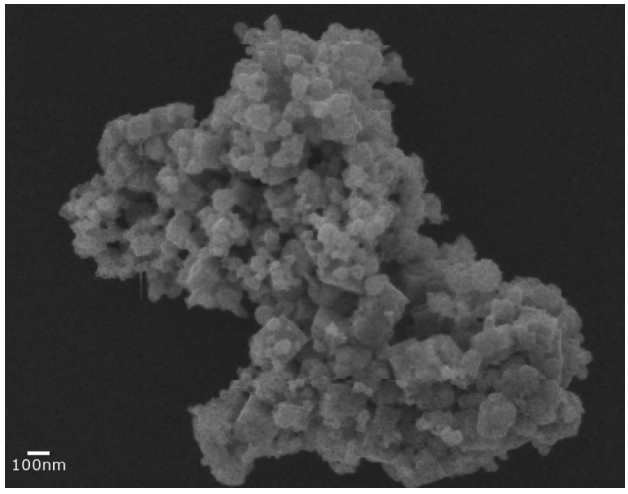

Figure 2. FE-SEM image of $BaTiO_3$ nanoparticles obtained by heat treatment at 140°C for 10 min in a microwave oven.

tetragonal nanoparticles, according with Kolen'ko et al.[30] These authors used a solvothermal method to study the cubic-tetragonal transition in nanopowders of barium titanate. They observed that samples with particle size smaller than 17 nm present only cubic structure, whereas samples with particles grown larger than this value have only tetragonal structures.

Figure 2 illustrates an FE-SEM image of the $BaTiO_3$ nanoparticles synthesized for 10 min, evidencing their nonuniform growth and particle distribution size in spherical morphology, which remained unaltered for all annealing times. The agglomeration process was attributed to Van der Waals forces. To reduce the surface energy, the primary particles have a tendency to form an agglomerate, by forming nearly spherical or equi-axed agglomerates, in a minimum surface to volume ratio and hence minimum surface free energy can be achieved.[31,32]

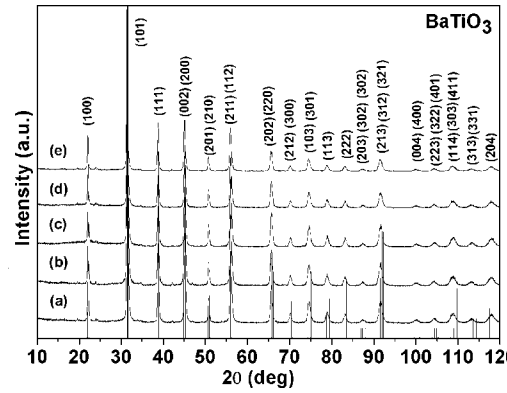

Figure 3. X-ray diffraction pattern of $BaTiO_3$ nanoparticles annealed at 140°C at (a) 10, (b) 20, (c) 40, (d) 80, and (e) 160 min in the HTMW system.

X-ray powder diffraction patterns of $BaTiO_3$ (BT) nanocrystalline particles are illustrated in Figure 3. Likewise, tetragonal $BaTiO_3$ (BT) nanoparticles were directly obtained from the hydrothermal microwave (HTMW) method. All peaks were indexed as a typical perovskite phase (JCPDS card no. 05-0626) with the *P*4*mm* space group in a tetragonal structure, besides an eventual tetragonal peak splitting of the reflections cannot be resolved due to overlapping on the (002) and (200) planes. A small amount of orthorhombic Witherite structure, with *Pmcn* space group, was identified as $BaCO_3$ and quantified by Rietveld refinements. Besides, the background of the diffractograms indicate a formation of a well-crystallized material, probably without a disordered secondary phase. The obtained results reveal that the chloride ions have an evident effect to enhance the formation of tetragonal $BaTiO_3$ under hydrothermal conditions as that reported by Ma, Dutta, and Gregg.[17,33] However, it shows a certain dependence on the synthesis route and temperature.

The fundamental parameters implemented in TOPAS ACADEMIC v4.1 software were used for the refinements.[29] The phase fractions found after the Rietveld refinement, demonstrated in Figure 4, were about 99.4% to tetragonal $BaTiO_3$ nanoparticles, with a *c*/*a* ratio at around 1.003 and less than 0.6% to the Witherite $BaCO_3$ phase. This image as a typical Rietveld analysis output can be used for the judgment of quality of the fitting. Thus, the obtained Rietveld refinement presents good agreement indexes,[29,34] where $R_{wp} = 11.92$ and 13.73, *R*-Bragg between 3.63 and 3.89, and χ^2 values for all patterns between 1.27 and 1.43.

Lee et al.[35] reported that OH^- ions are important in the nucleation of $BaTiO_3$ nanocrystals under hydrothermal condition. These ions also seemed to act as catalysts to accelerate the transition from Ba−OH bonds to $BaTiO_3$ crystals. Thus, the used concentration of KOH favored the formation of the barium titanate nanoparticles. Therefore, this nonthermic effect produces an increase in the diffusion rate and a decrease in the activation energy by molecule polarizations.[26] Ma et al.[17] assumed that the Cl^- ions favor

(30) Kolen'ko, Y. V.; Kovnir, K. A.; Neira, I. S.; Taniguchi, T.; Watanabe, T. T.; Sakamoto, N.; Yoshimura, M. *J. Phys. Chem. C.* **2007**, *111*, 7306.
(31) Khollam, Y. B.; Deshpande, A. S.; Patil, A. J.; Potdar, H. S.; Deshpande, S. B.; Date, S. K. *Mater. Chem. Phys.* **2001**, *71*, 304.
(32) Wilson, G. J.; Matijasevich, A. S.; Mitchell, D. R. G.; Schulz, J. C.; Will, G. D. *Langmuir* **2006**, *22*, 2016.
(33) Dutta, P. K.; Gregg, J. R. *Chem. Mater.* **1992**, *4*, 843.
(34) Moreira, M. L.; Pianaro, S. A.; Andrade, A. V. C.; Zara, A. J. *Mater. Charact.* **2006**, *57*, 193.
(35) Lee, S. K.; Park, T. J.; Choi, G. J. *Mater. Chem. Phys.* **2003**, *83*, 742.

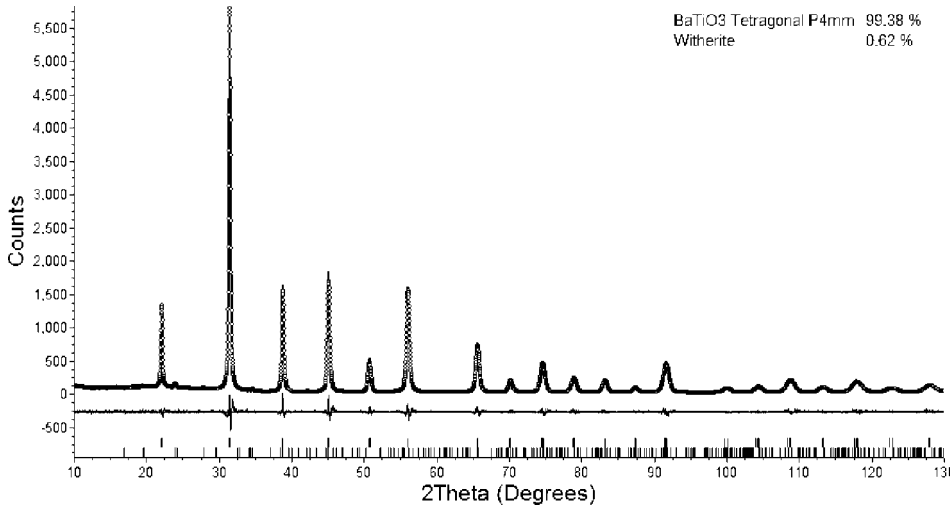

Figure 4. Rietveld refinement of $BaTiO_3$ nanoparticles synthesized by the HTMW method at 140°C for 10 min.

the tetragonal phase and thus might be associated with lattice strain and defects. To establish a phase stability diagram, we need to compute equilibrium concentrations of each species in a system as a function of temperature, pressure, pH, and the initial amount of reagents,[24] hence favoring the formation of $BaTiO_3$ nanoparticles at 140°C for 10 min by the hydrothermal microwave method under 2.5 bar pressure.

On the other hand, in accordance with Rabeneau et al., the water viscosity decreases with increasing temperature, and at 500 °C and 10 bar it is only 10% of its magnitude under ambient conditions. Under even more mild conditions, the viscosity is still lowered,[36] and thus it may be envisaged that the mobility of dissolved ions and molecules is higher under hydrothermal conditions than at ambient pressure and temperature taking into account the increase in the effective collision rate in solution during the hydrothermal microwave processing. This fact offers favorable thermodynamic conditions to the formation of the tetragonal barium titanate nanoparticles at low temperatures and short annealing times by the hydrothermal method. Besides, the use of electromagnetic microwave radiation acting directly on the permanent dipole of the water (rotational barriers) employs uniform ratings[32] and enhances by one or two orders of magnitude the kinetic crystallization behavior.[11,12]

The kinetics formation proposed to $BaTiO_3$ particles at 140 °C under rapid reacting from dilute (KOH 3 M) in aqueous solutions of $BaCl_2$ and $TiCl_4$ at pH 14 can be described by the overall reaction

$$BaCl_2(aq) + TiCl_4(aq) + 6KOH(aq) \rightarrow BaTiO_3(s) + 6KCl(aq) + 3H_2O(l) \quad (1)$$

The inductively coupled plasma atomic emission spectroscopy (ICP-AES) was used to determine the Ba/Ti ratio and determine the purity degree of the samples. To estimate the accuracy of the determinations in the $BaTiO_3$ solutions with lower salt concentrations, we prepared two series of 1:10 and 1:100 dilutions from the original digested samples. The dissolution procedure was carried out using 10 mL of HCl (37% m/m) and 3 mL of HNO_3 (68% m/m) in closed vessels at room temperature for 2 h. Analytical blanks were prepared following the same acid digestion procedure. Final sample solutions were made up to 100 mL with deionized water. Table 1 shows the nominal compositions of the powders. Then, following the present synthetic method to obtain barium titanate powders, a concentration of impurities (Ca + Sr + Mg) smaller than 1 ppm is achieved.

Table 1. Nominal and Analyzed (ICP) Compositions of $BaTiO_3$

ceramic denomination	composition (% molar fraction)	
	nominal	Analyzed[a]
$BaTiO_3$ samples	*x* Ba/Ti	*x* Ba/Ti
BT10 min	1	0.99 ± 0.006
BT20 min	1	0.98 ± 0.002
BT40 min	1	0.99 ± 0.004
BT80 min	1	1 ± 0.001
BT160 min	1	1 ± 0.002

[a] $n = 5$, average ± 1 sd, *x* is % molar fraction $BaTiO_3$.

A very large tetragonal distortion, $\delta = (c - a)/a = 6\%$, is commonly found to $PbTiO_3$, whereas for $BaTiO_3$, this amount equals only 1%; therefore, the angular resolution of peak-splitting is limited in particular for nanocrystalline materials. Vibrational spectroscopy, however, is sensitive to this type of transformation. This is in particular true for Raman spectroscopy, which can detect local lattice distortions and crystallographic defects at the molecular level.[37] Besides, all phonons of the cubic *Pm*3*m* symmetry are represented by $3F_{1u} + F_{2u}$, which include no Raman active normal modes.[38,39] Raman active modes of tetragonal $BaTiO_3$ powder in (*P*4*mm*) symmetry.[37–39] Electrostatic forces only reported in tetragonal symmetry induce the splitting of transverse and longitudinal phonons, resulting in split Raman active phonons represented by $3[A_1(TO) + A_1(LO)] + B_1 + 4[E(TO) + E(LO)]$.[39] The detailed phonon assignments are following for each one observed active modes: 720 cm^{-1} (E(4LO) + A_1(3LO)), 515 cm^{-1} (E(4TO) + A_1(3TO)), 305 cm^{-1} (E(3TO) + E(2LO) + B_1), 260 cm^{-1} (A_1(2TO)) and

(36) Rabeneau, A. *Angew. Chem., Int. Ed.* **1985**, *24*, 1026.

(37) Shiratori, Y.; Pithan, C.; Dornseiffer, J.; Waser, R. *J. Raman Spectrosc.* **2007**, *38*, 1288 Part I.

(38) Scalabrin, A.; Chaves, A. S.; Shim, D. S.; Porto, S. P. S. *Phys. Status Solidi* **1977**, *79*, 731.

(39) Nakamura, T.; Sakudo, T.; Ishibashi, Y.; Tominaga, Y. *Shokabo (Tokyo)* **1988**.

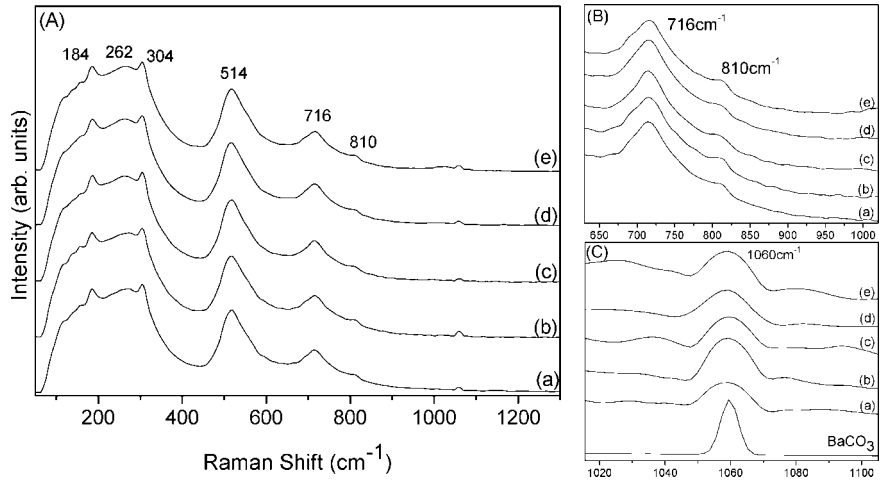

Figure 5. (A) Raman shift of tetragonal $BaTiO_3$ nanoparticles annealed at 140° for (a) 10, (b) 20, (c) 40, (d) 80, and (e) 160 min by HTMW system. (B) New vibrational mode at 810 cm^{-1} interpreted as a signal for disordered structure. (c) Peak related with barium carbonate.

185 cm^{-1} (E(2TO) + E(1LO) + $A_1$1TO) + A_1(1LO)).[40,41] All these vibrational modes can be clearly observed in Figure 5A.[40]

The appearance of a peak at 304 cm^{-1} in the samples indicates, at least at a local order, the asymmetry of TiO_6 octahedra within the $BaTiO_3$ structure. Hayashi et al.[42] reported that a peak around 310 cm^{-1} appeared below the Curie point and vanished above the Curie point in $BaTiO_3$ ceramics, suggesting that the peak at 304 cm^{-1} is an intrinsic peak for tetragonal $BaTiO_3$.

The 716 cm^{-1} related to the highest frequency longitudinal optical mode, besides the higher relative intensity of the band in comparison with the other tetragonal bands for nanoparticles can be related to Ba^{2+} defects in the $BaTiO_3$ lattice.[43] The peaks at 514, 262, and 184 cm^{-1} are assigned to the fundamental TO mode of A_1 symmetry while comprising the main difference in Raman spectra among tetragonal and orthorhombic phases of $BaTiO_3$.[37,44] The asymmetry in the peak at 515 cm^{-1} suggests the existence of coupling of TO modes associated with the tetragonal phase.[42] On the other hand, the peak at 184 cm^{-1} related with decoupling of the A_1(TO) phonons can be induced by phonon damping due to stress or lattice defects as well as the coexistence of the orthorhombic phase.[38,43] However, if the lattice remains tetragonal, then the stress and/or internal lattice defects can lead to random tilts in the TiO_6 octahedrons, because all these peaks are present in the Raman spectra of Figure 5A. Thus, these powders present a tetragonal structure that is in agreement with XRD and Rietveld refinement results.

Both X-ray diffraction and Raman spectroscopy techniques confirm the tetragonallity of $BaTiO_3$ nanoparticles. However, a new low-intensity vibrational mode at 810 cm^{-1}, as shown in Figure 5B, is interpreted as a signal of a disordered structure, because in that ICP report, no impurities contends to the samples. Thus, this vibrational mode at 810 cm^{-1} leads to the breakdown of the Raman selection rules by random substitution of cations, especially in highly polarized Ti ions and anion vacancies during the intermediate $BaTiO_3$ phase composition.[45] Shiratori and co-workers related this peak with the presence of OH^- lattice groups.[37] It is quite reasonable in our case because the samples were all grown in aqueous alkaline media. Figure 5C shows a small peak at 1060 cm^{-1} that appears in all spectra, besides the $BaCO_3$ spectrum in the same region. These results are in agreement with XRD measurements, confirming the presence of a small amount of the Witherite phase in all samples.

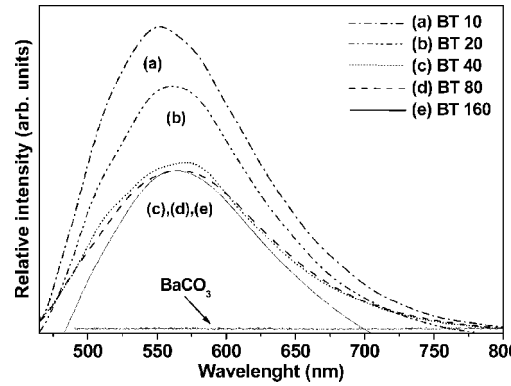

Figure 6. Photoluminescence of $BaTiO_3$ nanoparticles annealed at 140° for (a) 10, (b) 20, (c) 40, (d) 80, and (e) 160 min by the HTMW system.

Figure 6 presents the time evolution photoluminescence of $BaTiO_3$ nanoparticles synthesized by hydrothermal microwave method (HTMW). The photoluminescence profile is typical of a multiphonon process, i.e., the emission that occurs by several paths, involving numerous states within the band gap of the material.[46] The samples processed for

(40) Shiratori, Y.; Pithan, C.; Dornseiffer, J.; Waser, R. *J. Raman Spectrosc.* **2007**, *38*, 1288.
(41) Pontes, F. M.; Escote, M. T.; Escudeiro, C. C.; Leite, E. R.; Longo, E.; Chiquito, A. J.; Pizani, P. S.; Varela, J. A. *J. Appl. Phys.* **2004**, *96*, 4386.
(42) Hayashi, T.; Oji, N.; Maiwa, H. *Jpn. J. Appl. Phys.* **1994**, *33*, 5277.
(43) Busca, G.; Buscaglia, V.; Leoni, M.; Nanni, P. *Chem. Mater.* **1994**, *6*, 955.
(44) Joshi, U. A.; Yoon, S.; Baik, S.; Lee, J. S. *J. Phys. Chem. B.* **2006**, *110*, 25.
(45) Kumar, S.; Messing, G. L.; White, W. B. *J. Am. Ceram. Soc.* **1993**, *76*, 617.
(46) Anicete-Santos, M.; Cavalcante, L. S.; Orhan, E.; Paris, E. C.; Simões, L. G. P.; Joya, M. R.; Rosa, I. L. V.; Lucena, P. R.; de Santos, M. R. M. C.; Santos-Júnior, L. S.; Pizani, P. S.; Leite, E. R.; Varela, J. A.; Longo, E. *Chem. Phys.* **2005**, *316*, 260.

Table 2. Percent Area of Deconvolution $BaTiO_3$ Photoluminescence Bands

	percent area				
λ (nm)	$BaTiO_3$ 10min	$BaTiO_3$ 20min	$BaTiO_3$ 40min	$BaTiO_3$ 80min	$BaTiO_3$ 160min
504.2	8.80	8.72	7.96	7.10	6.81
537.8	28.16	26.82	25.93	22.70	22.60
579.8	29.56	30.46	31.61	33.95	34.07
626.3	33.46	33.98	34.48	36.23	36.50

10 and 20 min by the HTMW method present the maximum component emission around the green light range, with the maximum emission profile band centered at 556 and 559 nm, respectively. The samples heat treated for 40 (BT40), 80 (BT80), and 160 (BT160) min demonstrate a yellow-shift phenomenon, in which the maximum emission profile bands are centered at 564 nm for BT40, and 567 nm for BT80 and BT160. Figure 6 presents the PL analysis of the secondary phase $BaCO_3$. It is very important to observe that barium carbonate does not present photoluminescence properties and that the emission is due only to the $BaTiO_3$ phase.

To obtain a better understanding of the PL properties and their dependence on the structural order−disorder of the lattice, we analyzed the PL spectra using decomposition PeakFit,[47] based on the Gaussian line broadening mechanism for luminescence processes. A decrease in the Gaussian components in the green region and a respective increase in the components in the yellow wavelength can be observed as a function of increasing time. In this way, a reduction of the green emission occurs in detriment to the intrinsic yellow-shift for $BaTiO_3$ nanoparticles. Thus, $BaTiO_3$ nanoparticles indicate a trend to structural disorder when increasing the annealing time.[48,49] Table 2 shows the percentage of each component of photoluminescence behavior of samples. It is noted that both the excitation energy of 2.54 eV (488 nm) and maximum profile emission (2.2 eV) are smaller than the forbidden band gap energy of $BaTiO_3$ (3.57 eV).[50] Therefore, these results indicated that certain localized levels within the band gap must exist because the direct electron transition between the valence band and the conduction band should be not allowed. However, in this case,the involved states in the emission photoluminescence process originate from intrinsic defects of the crystalline material, because of a small amount of secondary phases (such as witherite, which is nonluminescent).

Thus, we are also inclined to ascribe the emission as an electron-hole recombination of a localized exciton Ti^3-O^- in a nonregular octahedron, due to d-orbital surface states stabilized in the forbidden gap.[51] Thus, the PL emission can be associated with structural disordered model to $BaTiO_3$ nanoparticles. This model is based on the octahedron tilt inside the cell, causing noticeable changes in the dihedral angle and hence altering the interaction among the electronic distributions on the atoms of the cell. This effect takes the formation of intermediate states inside the band gap. Other models presented by the literature allow such interpretation because of the observed modification of the electronic densities by the displacements from the primitive atomic positions to other ones.[52,53]

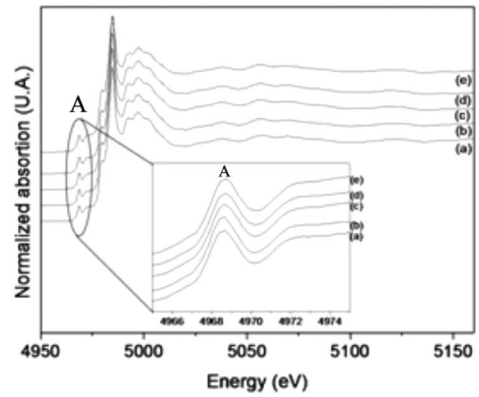

Figure 7. Results of Ti K-edge XANES spectra and (inset) normalized height of the pre-edge feature, for $BaTiO_3$ nanoparticles annealed at 140° for (a) 10, (b) 20, (c) 40, (d) 80, and (e) 160 min by the HTMW method.

It has been also reported in the literature that the intrinsic surface states and defects act as optical absorption centers, thus the intensity of the visible emission band will increase in particles with decreasing sizes.[2] Also, a decrease in the particle sizes will induce an increase in the forbidden band gap,[54,55] causing a large modification in the optical properties of TiO_2-based materials.[54] Therefore, the observed small increase in the forbidden band gap of 0.2 eV for $BaTiO_3$ nanoparticles from absorbance measurements was expected.

Figure 7 shows the Ti K-edge XANES spectra of barium titanate nanoparticles as a function of annealing time. All the spectra are very similar among themselves and are found in the literature for tetragonal $BaTiO_3$.[56] Therefore, the XANES spectra are in agreement with the Raman (Figure 5) and X-ray (Figure 3) results. The pre-edge feature A in the inset of Figure 7 is commonly attributed to the distortion of TiO_6 octahedron,[18] which in this case did not show a significant difference when the annealing time is changed. This means that in all the samples, titanium atoms are localized in a nonregular octahedron in the tetragonal structure of barium titanate.

The analysis of the XANES spectra also brings significant information about the titanium coordination geometry, showing that in this case there is no direct relationship between

(47) Ding, T.; Zheng, W. T.; Tian, H. W.; Zang, J. F.; Zhao, Z. D.; Yu, S. S.; Li, X. T.; Meng, F. L.; Wang, Y. M.; Kong, X. G. *Solid State Commun.* **2004**, *232*, 815.
(48) Pizani, P. S.; Leite, E. R.; Pontes, F. M.; Paris, E. C.; Rangel, J. H.; Lee, E. J. H.; Longo, E.; Delega, P.; Varela, J. A. *Appl. Phys. Lett.* **2000**, *77*, 824.
(49) Cavalcante, L. S.; Gurgel, M. F. C.; Simões, A. Z.; Longo, E.; Varela, J. A.; Joya, M. R.; Pizani, P. S. *Appl. Phys. Lett.* **2007**, *90*, 011901.
(50) Ianculescu, A.; Gartner, M.; Despax, B.; Bley, V.; Lebey, Th.; Gavrila, R.; Modreanu, M. *Appl. Surf. Sci.* **2006**, *253*, 344.
(51) Orhan, E.; Pontes, F. M.; Pinheiro, C. D.; Longo, E.; Pizani, P. S.; Varela, J. A.; Leite, E. R.; Boschi, T. M.; Beltrân, A.; Andrés, J. *J. Eur. Ceram. Soc.* **2005**, *25*, 2337.
(52) Cavalcante, L. S.; Gurgel, M. F. C.; Paris, E. C.; Simões, A. Z.; Joya, M. R.; Varela, J. A.; Pizani, P. S.; Longo, E. *Acta Mater.* **2007**, *55*, 6416.
(53) Xie, Y.; Yu, H.; Zhang, G.; Fu, H.; Sun, J. *J. Phys. Chem. C* **2007**, *111*, 6343.
(54) Meng, J.; Huang, Y.; Zhang, W.; Du, Z.; Zhu, Z.; Zou, G. *Phys. Lett. A* **1995**, *205*, 72.
(55) Venkatachalam, N.; Palanichamy, M.; Murugesan, V. *Mater. Chem. Phys.* **2007**, *104*, 454.
(56) Rumpf, H.; Modrow, H.; Hormes, J.; Glasel, H.; Hartmann, E.; Erdem, E.; Bo1ttcher, R.; Hallmeier, K. *J. Phys. Chem. B* **2001**, *105*, 3415.

TiO_5/TiO_6 units and the PL emission, in agreement with X-ray and Raman results. It seems that these local distortions around Ti atoms play an important role on the PL emission observed on the $BaTiO_3$ nanoparticles. However, complementary studies might be interesting in order to determine if this off-center disorder could be either static or dynamic.[57]

Another interesting point is that all used analytical techniques showed the formation of a tetragonal material. Raman spectroscopy showed a possible presence of OH lattice groups. To maintain charge equilibrium, some barium cations segregate in a secondary carbonate phase.[58] So, in our study, the photoluminescence properties are not related with a very disordered structure containing TiO_5 and TiO_6 clusters, like in some papers presented by our group.[59] Instead, this property can be related with lattice distortions such as tilted in the TiO_6 octahedron, caused by the presence of OH^- groups and Ba^{2+} vacancies. These two phenomena acting together are responsible for the formation of intermediary states inside the band gap, and, consequently, for the photoluminescence properties of the crystalline $BaTiO_3$ samples.

Conclusions

From the above results and discussion, it is clear that tetragonal $BaTiO_3$ nanocrystalline powders were directly crystallized from hydrothermal microwave method, using rapid reacting, chlorides as precursor salts, and KOH as a mineralizer, which provide favorable conditions to synthesize the tetragonal BT phase. The Rietveld refinements provide great agreement index parameters, confirming the tetragonal structure of the $BaTiO_3$ nanoparticles, and a small amount of carbonate, which decisively did not contribute to other results. In agreement with X-ray diffraction powders, the Raman and XANES spectra confirm the tetragonally of the samples indicating a non-regular octahedron formation in the structure by the presence of hydroxyl groups and Ba^{2+} vacancies. The yellow-shift PL emission is corroborated by the slight increase of the Ti pre-edge "A" from XANES spectroscopy, indicating a larger disorder in the octahedron for the BT160 sample than BT10 sample. Therefore, the HTMW method is undeniably a genuine technique for low temperatures and short times in comparison with the above mentioned methodologies. Thus, we are inclined to believe these are the main reason for the existence of the photoluminescence emission in the $BaTiO_3$ nanoparticles.

Acknowledgment. The authors acknowledge the support of Brazilian agencies CAPES, CNPq, and FAPESP. TEM and FE-SEM and XANES facilities were provided by LNLS, Campinas, SP, Brazil.

CM801638D

(57) Ravel, B.; Stern, E. A.; Vedrinski, R. I.; Kraizman, V. *Ferroelectrics* **1998**, *206* (1−4), 407.
(58) Sun, W.; Pang, Y.; Li, J.; Ao, W. *Chem. Mater.* **2007**, *19*, 1772.
(59) Paris, E. C.; Espinosa, J. W. M.; de lazaro, S.; Lima, R. C.; Joya, M. R.; Pizani, P. S.; Leite, E. R.; Souza, A. G.; Varela, J. A.; Longo, E. *Chem. Phys.* **2007**, *335* (1), 7.